Antimycin A induces death of the human pulmonary fibroblast cells via ROS increase and GSH depletion

WOO HYUN PARK and BO RA YOU

Department of Physiology, Medical School, Research Institute for Endocrine Sciences, Chonbuk National University, Jeonju 561-180, Republic of Korea

Received October 6, 2015; Accepted November 20, 2015

DOI: 10.3892/ijo.2015.3276

Abstract. Antimycin A (AMA) inhibits the growth of various cells via stimulating oxidative stress-mediated death. However, little is known about the anti-growth effect of AMA on normal primary lung cells. Here, we investigated the effects of AMA on cell growth inhibition and death in human pulmonary fibroblast (HPF) cells in relation to reactive oxygen species (ROS) and glutathione (GSH) levels. AMA inhibited the growth of HPF cells with an IC_{50} of ~150 μM at 24 h. AMA induced a G1 phase arrest of the cell cycle and it also triggered apoptosis accompanied by the loss of mitochondrial membrane potential (MMP; $\Delta\Psi_m$). AMA increased ROS levels including $O_2\cdot$- in HPF cells from the early time point of 25 min. It induced GSH depletion in HPF cells in a dose-dependent manner. Z-VAD (a pan-caspase inhibitor) did not significantly prevent cell death and MMP ($\Delta\Psi_m$) loss induced by AMA. N-acetylcysteine (NAC; an antioxidant) attenuated cell growth inhibition, death and MMP ($\Delta\Psi_m$) loss in AMA-treated HPF cells and NAC generally decreased the ROS level in these cells as well. Vitamin C enhanced cell growth inhibition, death, GSH depletion and $O_2\cdot$- levels in 100 μM AMA-treated HPF cells whereas this agent strongly attenuated these effects in 200 μM AMA-treated cells. In conclusion, AMA inhibited the growth of HPF cells via apoptosis as well as a G1 phase arrest of the cell cycle. AMA-induced HPF cell death was related to increased ROS levels and GSH depletion.

Correspondence to: Professor Woo Hyun Park, Department of Physiology, Medical School, Chonbuk National University, Jeonju 561-180, Republic of Korea
E-mail: parkwh71@jbnu.ac.kr

Abbreviations: HPF, human pulmonary fibroblast; AMA, antimycin A; ROS, reactive oxygen species; MMP ($\Delta\Psi_m$), mitochondrial membrane potential; SOD, superoxide dismutase; CAT, catalase; GSH, glutathione; GPX, GSH peroxidase; TXN, thioredoxin; TXNR, TXN reductase; H_2DCFDA, 2',7'-dichlorodihydrofluorescein diacetate; DHE, dihydroethidium; CMFDA, 5-chloromethylfluorescein diacetate; NAC, N-acetylcysteine; BSO, L-buthionine sulfoximine

Key words: human pulmonary fibroblast, antimycin A, cell death, reactive oxygen species, glutathione

Introduction

Reactive oxygen species (ROS) such as hydrogen peroxide (H_2O_2), superoxide anion ($O_2\cdot$-) and hydroxyl radical ($\cdot$OH) are involved in diverse cellular proceedings of differentiation, cell proliferation and cell death. Redox status changes in tissues and cells influence the production and metabolism of ROS. ROS are primarily generated during the mitochondrial respiration and are specifically made by various oxidases (1). Superoxide dismutases (SODs) [cytoplasmic (SOD1), mitochondrial (SOD2) or extracellular (SOD3) isoforms] metabolize $O_2\cdot$- to H_2O_2 (2). Further metabolism of H_2O_2 by catalase (CAT) or glutathione (GSH) peroxidase (GPX) yields O_2 and H_2O (3). Particularly, thioredoxin (TXN) system consisting of TXN, TXN reductase (TXNR) and NADPH critically regulates cellular redox homeostasis (4). TXN as a thiol reductase acts as a potent anti-oxidant as well as a scavenger against ROS (4). Oxidative stress due to either overproduction of ROS or accumulation of them can initiate events that lead to cell death.

Antimycin A (AMA) derived from *Streptomyces kitazawensis* inhibits succinate and NADH oxidases and this agent also impedes mitochondrial electron transport via its binding to complex III (5). The inhibition of electron transport triggers a failure of the proton gradient across the mitochondrial inner membrane, thereby collapsing mitochondrial membrane potential (MMP; $\Delta\Psi_m$) (6,7). This inhibition can lead to the overproduction of ROS (7,8). Accordingly, oxidative stress and the collapse of MMP ($\Delta\Psi_m$) by AMA unlock the mitochondrial permeability transition pore (PTP), which is accompanied by the release of cytochrome *c* into the cytoplasm to induce apoptosis (9,10). In fact, AMA-induced apoptosis has been reported in a variety of cells including HeLa cervical cancer cells (11), As4.1 juxtaglomerular cells (12), HL60 leukemia cells (13) and Hep3B hepatoma cells (14) and normal endothelial cells (15).

Previously we reported that AMA reduces the growth of Calu-6 and A549 lung cancer cells via apoptosis and cell cycle arrest (16,17). AMA also increases ROS levels in A549 cells (17) and induces GSH depletion in Calu-6 cells (18). However, little is known about the cellular effects of PG on normal primary lung cells. Thus, we examined the effects of AMA on cell growth and death in human pulmonary fibroblast (HPF) cells in relation to ROS and GSH levels. In addition, we investigated the effects of N-acetylcysteine (NAC) and vitamin C

(well known antioxidants) or L-buthionine sulfoximine (BSO; an inhibitor of GSH synthesis) on AMA-induced HPF cell death.

Materials and methods

Cell culture. HPF cells purchased from PromoCell GmbH (Heidelberg, Germany) were cultured in RPMI-1640 supplemented with 10% fetal bovine serum (FBS) and 1% penicillin-streptomycin (Gibco BRL, Grand Island, NY, USA). HPF cells were used for experiments between passages four and eight.

Reagents. AMA purchased from Sigma-Aldrich Chemical Co. was dissolved in ethanol at 20 mM. Pan-caspase inhibitor (Z-VAD-FMK) was obtained from R&D Systems, Inc. (Minneapolis, MN, USA) and was dissolved in dimethyl sulfoxide (Sigma-Aldrich Chemical Co.). NAC and BSO were obtained from Sigma-Aldrich Chemical Co. NAC was dissolved in the buffer [20 mM HEPES (pH 7.0)]. BSO was dissolved in water. Vitamin C purchased from Riedel-de Haen (Hannover, Germany) was also dissolved in water. Based on the previous studies (19,20), cells were pretreated with or without 15 μM Z-VAD, 2 mM NAC, 10 μM BSO or 1 mM vitamin C for one hour prior to AMA treatment.

Cell growth inhibition assays. Cell growth changes were determined by measuring the 3-(4,5-dimethylthiazol-2-yl)-2,5-diphenyltetrazolium bromide (MTT, Sigma-Aldrich Chemical Co.) dye absorbance as previously described (21). Cells were exposed to the indicated amounts of AMA (2-200 μM) with or without Z-VAD, NAC, vitamin C or BSO for 24 h.

Cell cycle and sub-G1 analysis. Cell cycle and sub-G1 cells were determined by propidium iodide (PI, Ex/Em=488 nm/617 nm; Sigma-Aldrich) staining as previously described (22). Cells were incubated with the indicated amounts of AMA (2-200 μM) for 24 h. Cellular DNA content was measured using a FACStar flow cytometer (Becton-Dickinson, Franklin Lakes, NJ, USA).

Annexin V/PI staining for cell death detection. Apoptosis was determined by staining cells with Annexin V-fluorescein isothiocyanate (FITC, Ex/Em=488 nm/519 nm; Invitrogen Molecular Probes, Eugene, OR, USA) and propidium iodide (PI, Ex/Em=488 nm/617 nm; Sigma-Aldrich), as previously described (22). Cells were incubated with the indicated amounts of AMA (2-200 μM) in the presence or absence of Z-VAD, NAC, vitamin C or BSO for 24 h. Annexin V/PI staining was analyzed with a FACStar flow cytometer (Becton-Dickinson).

Western blot analysis. The changes of proteins related to apoptosis and antioxidant system were determined by western blotting as previously described (22). Cells were incubated with 150 μM AMA for 24 h. Samples containing 10 μg total protein were resolved by 12.5% SDS-PAGE gels, transferred to Immobilon-P PVDF membranes (Millipore, Billerica, MA, USA) by electroblotting and then probed with anti-PARP, anti-SOD1, anti-SOD2, anti-procaspase-3, anti-TXN, anti-TXNR1, anti-TXNR2 and anti-β-actin antibodies (Santa Cruz Biotechnology, Santa Cruz, CA, USA).

Measurement of MMP ($\Delta\Psi_m$). MMP ($\Delta\Psi_m$) levels were measured using a rhodamine 123 fluorescent dye (Sigma-Aldrich; Ex/Em=485 nm/535 nm) as previously described (21,22). Cells were incubated with the indicated amounts of AMA (2-200 μM) in the presence or absence of Z-VAD, NAC, vitamin C or BSO for 24 h. The absence of rhodamine 123 from cells indicated the loss of MMP ($\Delta\Psi_m$) in HPF cells. The MMP ($\Delta\Psi_m$) levels in the cells excluding MMP ($\Delta\Psi_m$) loss cells were expressed as mean fluorescence intensity (MFI), which was calculated by CellQuest software (Becton-Dickinson).

Detection of intracellular ROS levels. Intracellular ROS were detected by a fluorescent probe dye, 2',7'-dichlorodihydro-fluorescein diacetate (H_2DCFDA, Ex/Em=495 nm/529 nm; Invitrogen Molecular Probes) as previously described (22). Dihydroethidium (DHE, Ex/Em=518 nm/605 nm; Invitrogen Molecular Probes) is a fluorogenic probe that is highly selective for $O_2^{\cdot -}$ among ROS. Cells were incubated with the indicated doses of AMA (2-200 μM) in the presence or absence of Z-VAD, NAC, BSO or vitamin C for the indicated times. The fluorescence of DCF and DHE was detected using a FACStar flow cytometer (Becton-Dickinson). ROS levels were expressed as MFI.

Detection of the intracellular GSH. Cellular GSH levels were analyzed using a 5-chloromethylfluorescein diacetate dye (CMFDA, Ex/Em=522 nm/595 nm; Invitrogen Molecular Probes) as previously described (21,22). Cells were incubated with the indicated doses of AMA (2-200 μM) in the presence or absence of Z-VAD, NAC, BSO or vitamin C for the indicated times. CMF fluorescence intensity was determined using a FACStar flow cytometer (Becton-Dickinson). Negative CMF staining (GSH depleted) cells were expressed as the percent of (-) CMF cells.

Statistical analysis. The results correspond to the mean of three independent experiments (mean ± SD). The data were analyzed using Instat software (GraphPad Prism4, San Diego, CA, USA). The Student's t-test or one-way analysis of variance (ANOVA) with post hoc analysis using Tukey's multiple comparison test was used for parametric data. Statistical significance was defined as $p<0.05$.

Results

Effects of AMA on cell growth and cell cycle distribution in HPF cells. Firstly, we investigated the effect of AMA on the growth of HPF cells at 24 h. Based on MTT assays, AMA decreased HPF cell growth with an IC_{50} of ~150 μM in a dose-dependent manner (Fig. 1A). When cell cycle distributions was examined in AMA-treated HPF cells, AMA induced a G1 phase arrest of the cell cycle as compared with control cells (Fig. 1B). Furthermore, 200 μM AMA clearly increased the number of sub-G1 DNA content cells by ~10% as compared with that of control HPF cells (Fig. 1B). However, other doses of AMA did not increase the number of sub-G1 DNA content cells (Fig. 1B).

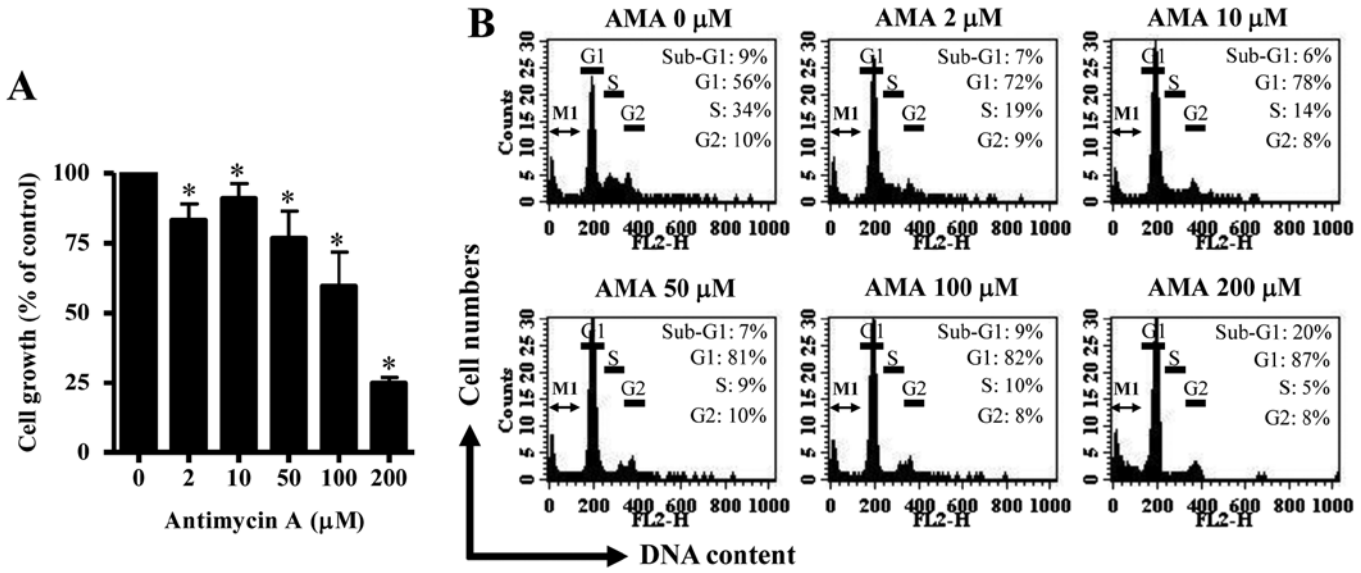

Figure 1. Effects of AMA on cell growth and cell cycle distributions in HPF cells. (A) The graph shows cellular growth changes in HPF cells. (B) Each histogram shows the cell cycle distributions in HPF cells. M1 indicates sub-G1 cells in each histogram. *p<0.05 compared with the control group.

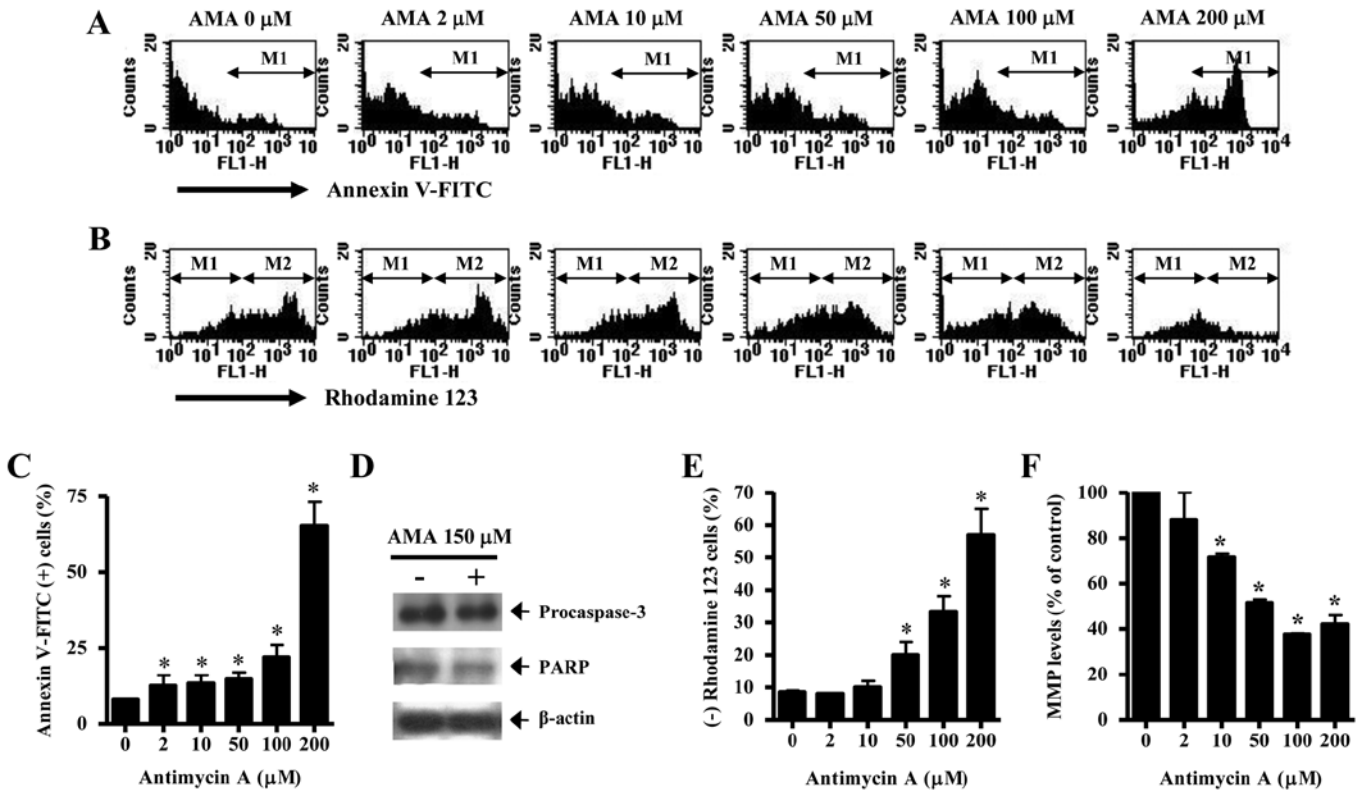

Figure 2. Effects of AMA on cell death and MMP ($\Delta\Psi_m$) in HPF cells. (A and B) Annexin V-FITC and rhodamine 123 staining cells were measured by FACStar flow cytometer, respectively. M1 regions in the histograms (A) indicate Annexin V-FITC-positive cells. M1 and M2 regions in the histograms (B) indicate rhodamine 123-negative and positive cells, respectively. (C) The graph shows the percents of Annexin V-FITC cells in HPF cells from (A). (D) Samples of protein extracts (10 μg) were resolved by SDS-PAGE gel, transferred onto PVDF membranes and immunoblotted with the indicated antibodies against procaspase-3, PARP and β-actin. (E and F) Graphs show the percent of rhodamine 123-negative [M1 region (B); MMP ($\Delta\Psi_m$) loss] cells (E) and MMP ($\Delta\Psi_m$) levels [M2 region (B)] in the cells (F). *p<0.05 compared with the control group.

Effects of AMA on cell death, apoptosis-related proteins and MMP ($\Delta\Psi_m$) in HPF cells. It was determined whether AMA induces HPF cell death via apoptosis. As shown in Fig. 2A and C, AMA increased the numbers of Annexin V-FITC-positive cells in a dose-dependent manner. The elevated change was observed between 100 and 200 μM AMA treatment (Fig. 2A and C). Western blotting showed that a 32-kDa precursor (procaspase-3) slightly disappeared in AMA-treated

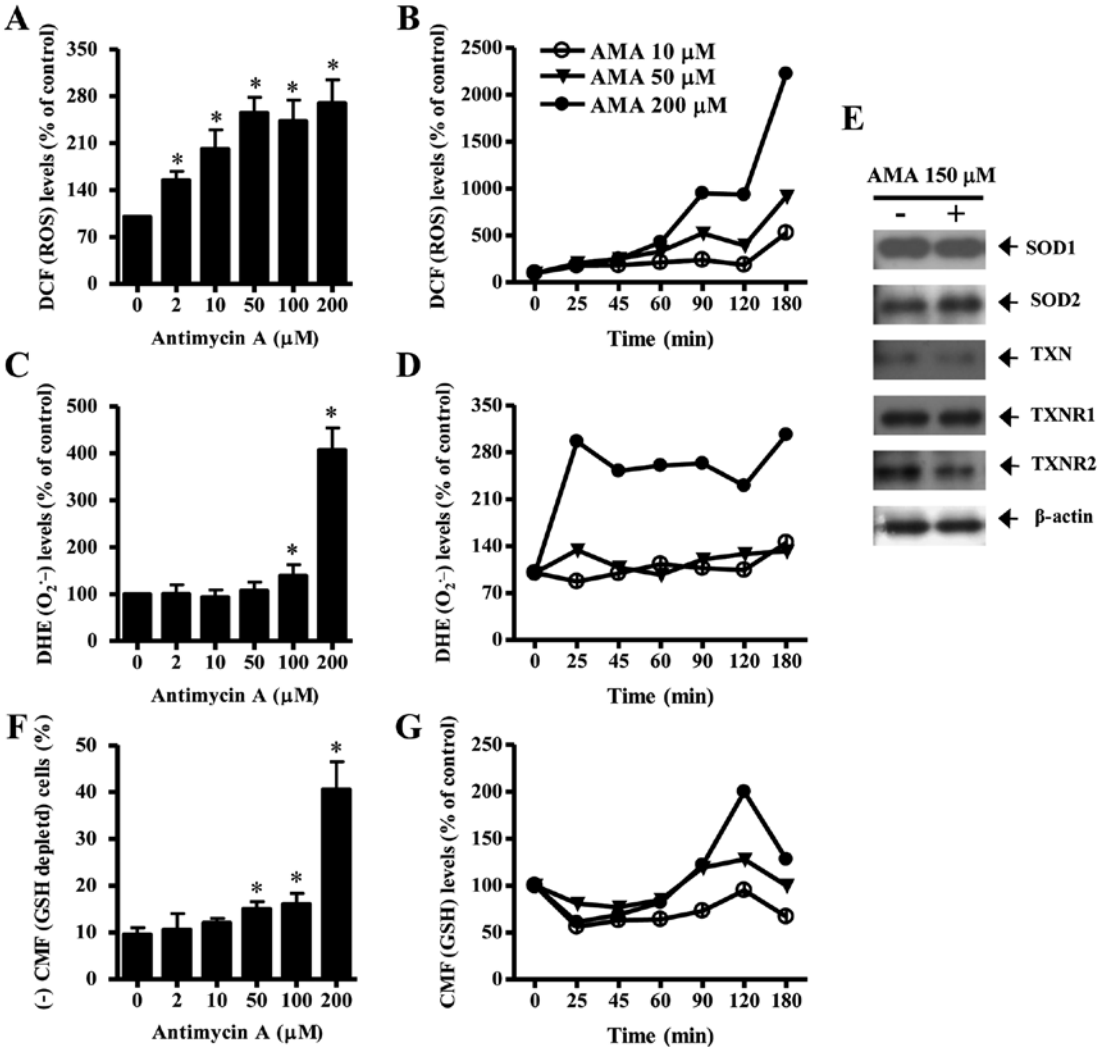

Figure 3. Effects of AMA on ROS and GSH levels in HPF cells. Intracellular GSH and ROS levels were measured using a FACStar flow cytometer. (A and B) Graphs indicate DCF (ROS) levels (%) in HPF cells at 24 h (A) and at the early times (B). (C and D) Graphs indicate DHE (O_2·-) levels (%) in HPF cells at 24 h (C) and at the early times (D). (E) Samples of protein extracts (10 μg) were resolved by SDS-PAGE gels, transferred onto PVDF membranes and immunoblotted with the indicated antibodies against SOD1, SOD2, TXN, TXNR1, TXNR2 and β-actin. (F and G) Graphs show (-) CMF (GSH-depleted) cells (%) at 24 h (F) and GSH levels at the early times (G). *p<0.05 compared with the control group.

HPF cells, implying that caspase-3 was activated in these cells (Fig. 2D). The intact 116 kDa moiety of poly(ADP-ribose) polymerase (PARP) was decreased by AMA (Fig. 2D). Apoptosis is closely related to the collapse of MMP ($\Delta\Psi_m$). Correspondingly, 50-200 μM AMA significantly induced the loss of MMP ($\Delta\Psi_m$) in HPF cells (Fig. 2B and E). The percentage of MMP ($\Delta\Psi_m$) loss in 50 or 100 μM AMA-treated HPF cells was higher than those of Annexin V-FITC-positive cells in these cells (Fig. 2A-C and E). The levels of MMP ($\Delta\Psi_m$) in HPF cells excluding MMP ($\Delta\Psi_m$) loss cells were decreased by AMA in a dose-dependent manner (Fig. 2F).

Effects of AMA on ROS, GSH and antioxidant-protein levels in HPF cells. To assess intracellular ROS and GSH levels in AMA-treated HPF cells, we used H_2DCFDA, DHE and CMF dyes. As shown in Fig. 3A, all the tested doses of AMA significantly increased ROS (DCF) levels in HPF cells at 24 h. Moreover, 10-200 μM AMA gradually increased ROS (DCF) levels from 25 min to 180 min although there was a transient decrease in ROS level at 120 min (Fig. 3B). At 180 min, 200 μM AMA tremendously augmented ROS (DCF) level in HPF cells. Intracellular O_2·- (DHE) level was significantly increased in 100 or 200 μM AMA-treated HPF cells at 24 h whereas the level was not clearly changed at the treatment of 2, 10 or 50 μM AMA (Fig. 3C). Treatment with 50 and 200 μM AMA transiently increased O_2·- level in HPF cells at 25 min whereas 10 μM AMA decreased the level at this time (Fig. 3D). At 180 min, all the tested doses of AMA increased O_2·- levels in HPF cells and 200 μM AMA showed a strong effect (Fig. 3D). There was also a transient decrease in O_2·- level in 200 μM AMA-treated HPF cells at 120 min (Fig. 3D). When antioxidant-protein levels were assessed in 150 μM AMA-treated HPF cells, the expression of SOD1 was not changed by AMA and SOD2 was slightly increased (Fig. 3E). In addition, AMA downregulated the expression of TXN and TXNR2 in HPF cells and it did not change that of TXNR1 (Fig. 3E).

Treatment with 50, 100 or 200 μM AMA significantly increased GSH depleted cell number in HPF cells (Fig. 3F). However, the lower doses of 2 or 10 μM AMA did not induce

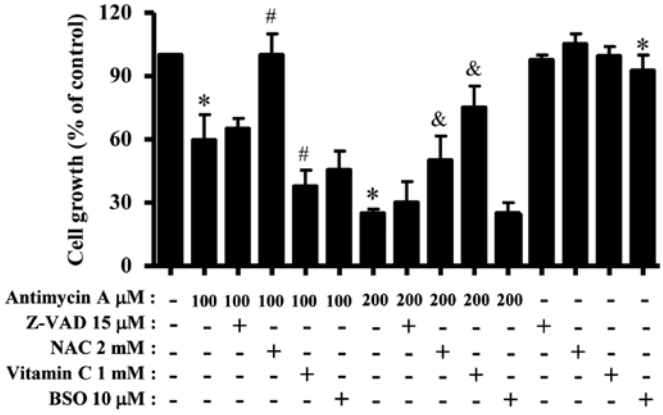

Figure 4. Effects of Z-VAD, NAC, vitamin C or BSO on cell growth in AMA-treated HPF cells. The graph shows cell growth changes in HPF cells as assessed by MTT assays. *p<0.05 compared with the control group. #p<0.05 compared with cells treated with 100 μM AMA. &p<0.05 compared with cells treated with 200 μM AMA.

GSH depletion in HPF cells as compared with control HPF cells (Fig. 3F). At the early time-points of 25-90 min, all the doses of AMA reduced GSH content level in HPF cells (Fig. 3G). There were increases in GSH levels in AMA-treated HPF cells at 120 min and the increases were attenuated at 180 min (Fig. 3G).

Effects of Z-VAD, NAC, vitamin C or BSO on cell growth, cell death and MMP ($\Delta\Psi_m$) in AMA-treated HPF cells. We examined the effect of Z-VAD, NAC, vitamin C and BSO on the growth and death of AMA-treated HPF cells. For this experiment, 100 or 200 μM AMA was used as a suitable dose to differentiate the levels of cell growth inhibition and death. Treatment with 15 μM Z-VAD slightly attenuated growth inhibition in AMA-treated HPF cells (Fig. 4). NAC strongly attenuated HPF cell growth inhibition by 100 or 200 μM AMA (Fig. 4). Vitamin C significantly enhanced cell growth inhibition in 100 μM AMA-treated HPF cells but this agent strongly prevented that in 200 μM AMA-treated HPF cells (Fig. 4). BSO slightly increased HPF cell growth inhibition by 100 μM AMA but it did not affect that in 200 μM AMA-treated HPF cells (Fig. 4). BSO alone slightly inhibited HPF control cell growth (Fig. 4).

In relation to cell death and the loss of MMP ($\Delta\Psi_m$), Z-VAD did not significantly influence HPF cell death by 100 or 200 μM AMA (Fig. 5A and B). NAC significantly attenuated apoptosis in 100 or 200 μM AMA-treated HPF cells

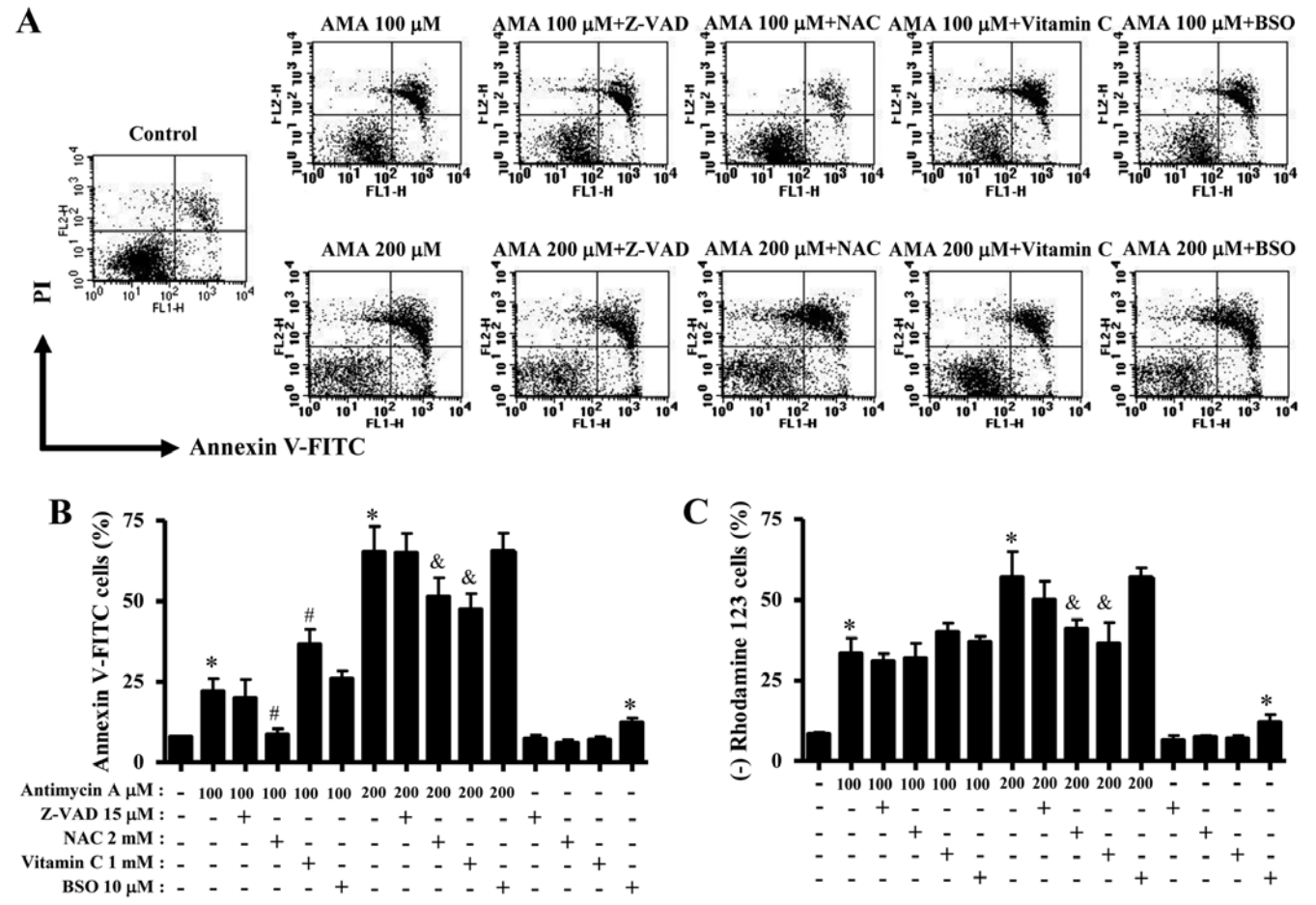

Figure 5. Effects of Z-VAD, NAC, vitamin C or BSO on cell death and MMP ($\Delta\Psi_m$) in AMA-treated HPF cells. (A) Each figure shows Annexin V-FITC/PI cells. (B and C) Graphs show the percents of Annexin V-positive staining cells from A, (B) and rhodamine 123-negative [MMP ($\Delta\Psi_m$) loss] cells (C). *p<0.05 compared with the control group. #p<0.05 compared with cells treated with 100 μM AMA. &p<0.05 compared with cells treated with 200 μM AMA.

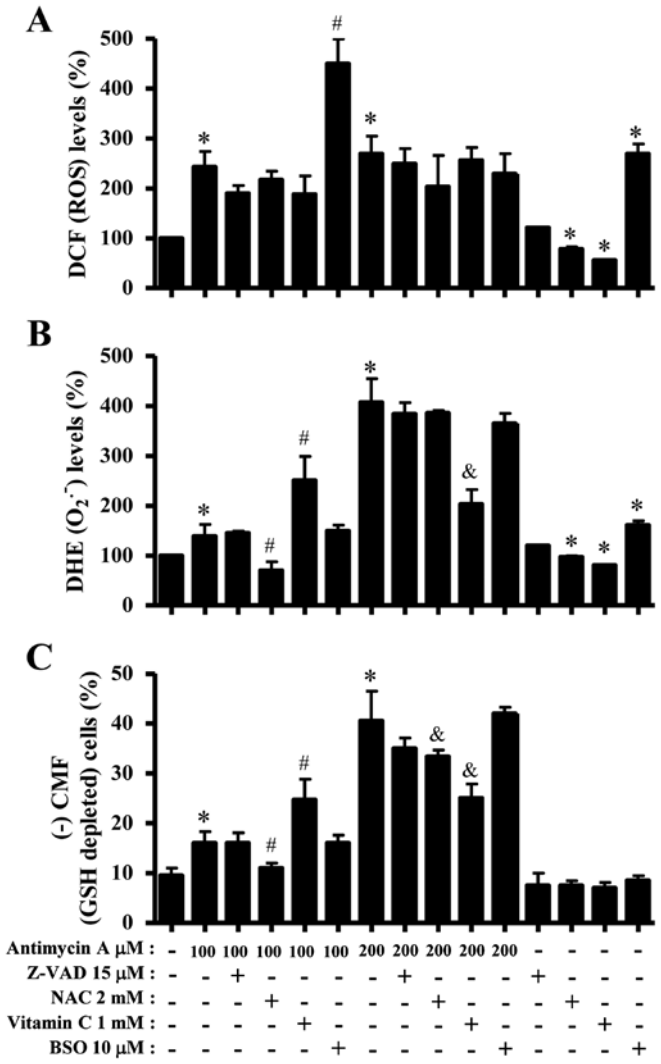

Figure 6. Effects of Z-VAD, NAC, vitamin C or BSO on ROS and GSH levels in AMA-treated HPF cells. (A-C) Graphs indicate ROS (as determined by DCF) levels (%) (A), DHE ($O_2^{\cdot-}$) levels (%) (B) and (-) CMF (GSH-depleted) cells (%) (C). *p<0.05 compared with the control group. #p<0.05 compared with cells treated with 100 μM AMA. &p<0.05 compared with cells treated with 200 μM AMA.

(Fig. 5A and B). However, NAC did not increase the number of viable (Annexin V-negative and PI-negative) cells in 200 μM AMA-treated HPF cells but it increased that of necrotic (Annexin V-negative and PI-positive) cells in these cells (Fig. 5A). While vitamin C enhanced apoptosis in 100 μM AMA-treated HPF cells, this agent significantly prevented that by 200 μM AMA (Fig. 5A and B). BSO mildly enhanced HPF cell death by 100 μM AMA, but not 200 μM AMA (Fig. 5A and B). BSO alone induced HPF control cell death (Fig. 5B). Moreover, Z-VAD and NAC did not change the loss of MMP ($\Delta\Psi_m$) in 100 μM AMA-treated HPF cells whereas vitamin C and BSO seemed to increase the loss in these cells (Fig. 5C). In 200 μM AMA-treated HPF cells, Z-VAD, NAC and vitamin C decreased the loss of MMP ($\Delta\Psi_m$) (Fig. 5C). BSO did not affect the loss of MMP ($\Delta\Psi_m$) in these cells and it alone induced the loss in HPF control cells (Fig. 5C).

Effects of Z-VAD, NAC, vitamin C or BSO on ROS and GSH levels in AMA-treated HPF cells. Next, ROS and GSH levels in 100 or 200 μM AMA-treated HPF cells were assessed in the presence or absence of Z-VAD, NAC, vitamin C or BSO. As shown in Fig. 6A, Z-VAD, NAC or vitamin C seemed to decrease ROS (DCF) levels in 100 or 200 μM AMA-treated or -untreated HPF cells. BSO strongly enhanced the levels in 100 μM AMA-treated or -untreated HPF cells but it decreased those in 200 μM AMA-treated HPF cells (Fig. 6A). Z-VAD did not significantly affect $O_2^{\cdot-}$ level in 100 μM AMA-treated HPF cells whereas NAC strongly decreased $O_2^{\cdot-}$ level in these cells (Fig. 6B). Vitamin C increased $O_2^{\cdot-}$ level in 100 μM AMA-treated HPF cells, but BSO did not change the level in these cells (Fig. 6B). In 200 μM AMA-treated HPF cells, Z-VAD, NAC, vitamin C and BSO decreased $O_2^{\cdot-}$ levels and vitamin C-treated group had a significant effect (Fig. 6B). NAC and vitamin C reduced basal $O_2^{\cdot-}$ level in HPF control cells whereas BSO increased the level (Fig. 6B). In relation to GSH levels, NAC significantly decreased GSH depleted cell number in 100 μM AMA-treated HPF cells whereas vitamin C increased the number in these cells (Fig. 6C). Z-VAD and BSO did not affect the cell number (Fig. 6C). In 200 μM AMA-treated HPF cells, Z-VAD, NAC, vitamin C and BSO decrease GSH depleted cell number and NAC or vitamin C-treated groups showed significant effects (Fig. 6C).

Discussion

We demonstrated the molecular mechanism of AMA on HPF cell growth inhibition and death in relation to ROS and GSH levels. AMA dose-dependently decreased HPF cell growth with an IC_{50} of ~150 μM. According to our previous reports (16,17), the IC_{50}s of AMA in A549 and Calu-6 lung cancer cells were ~2 and 100 μM at 24 h, respectively. Therefore, HPF cells seemed to be more resistant to AMA than the lung cancer cells of A549 and Calu-6. In addition, calf normal pulmonary artery endothelial cells were more resistant to AMA than Calu-6 cells (16). Since the activity of mitochondria is associated with a susceptibility to apoptosis (23), the difference of susceptibility to AMA among various different cancer and normal cell lines probably is due to the different basal activities of antioxidant enzymes and mitochondria each cell possesses. Furthermore, we observed that AMA altered the levels of SOD2 and TXNR2, which are specifically expressed in mitochondria to eliminate ROS.

Suppression of cell growth due to AMA can be explained in part by its capacity to affect the arrest during the cell cycle. For instances, 100 μM AMA inhibited HPF cell growth by >40% whereas this concentration increased the percentage of Annexin V staining cells by ≤10% as compared with the control cells. Therefore, G1 phase arrest of the cell cycle in AMA-treated HPF cells was considered as a pathway to suppress their growth. Similarly, AMA induces a G1 phase arrest in A549 and Calu-6 cells (16,17). On the other hand, AMA induces the S phase arrest in HeLa cells (24) and non-specifically induces the arrest in all the phases in As4.1 juxta-glomerular cells (25). These results suggest that the inhibition of mitochondrial electron transport by AMA can alter the cell cycle progression and the specificity of cell cycle arrest depends on differences in cell types. In addition, 2-100 μM AMA showing HPF cell growth inhibition did not increase the portion of sub-G1 DNA content cells but these doses increased

The Annexin V staining cell number. These results supported the notion that Annexin V staining cells are a marker to detect early apoptotic cells ahead of observing the sub-G1 cells.

AMA induces the collapse of MMP ($\Delta\Psi_m$) during apoptosis in various cells including cancer cells (11,12,15-17). Likewise, AMA induced the loss of MMP ($\Delta\Psi_m$) in HPF cells and decreased its level in the viable HPF cells. Particularly, the percentage of MMP ($\Delta\Psi_m$) loss by 50 or 100 μM AMA was higher than those of Annexin V-FITC-positive cells, implying that AMA primarily damages the mitochondria function in HPF cells, resulting in the loss of MMP ($\Delta\Psi_m$) and consequently induction of apoptosis. The activation of caspase-3 and the cleavage of PARP protein are known to be essential in AMA-induced cell death (16). According to our results, AMA increased caspase-3 activity and decreased PARP protein in HPF cells. Z-VAD slightly attenuated growth inhibition and MMP ($\Delta\Psi_m$) loss in 100 μM AMA-treated HPF cells. However, Z-VAD did not prevent HPF cell death from AMA insult. Therefore, caspase activation was not tightly related to AMA-induced HPF apoptosis but its activation partially affected cell growth and mitochondria. Our previous report demonstrated that 15 μM Z-VAD including other caspase inhibitors significantly prevented apoptosis in AMA-treated Calu-6 cells (16). It is possible that the dose of 15 μM Z-VAD was not enough to prevent AMA-induced HPF cell death because the mechanism of cell death can be different between cancer and normal cells.

AMA can disturb the natural oxidation/reduction equilibrium in various cells via causing a breakdown in MMP ($\Delta\Psi_m$). AMA increases ROS levels in HeLa cells (11), endothelial cells (15), As4.1 juxtaglomerular cells (25) and A549 cells (8,17). Likewise, ROS levels (as determined by DCF) were dose-dependently increased in AMA-treated HPF cells at 24 h and ROS levels were also strongly increased at the earlier time-point of 25 min. In addition, $O_2\cdot$- level (as determined by DHE) was increased in AMA-treated HPF cells. Especially, 200 μM AMA strongly augmented $O_2\cdot$- level in HPF cells as compared with 100 μM AMA-treated cells. In addition, 200 μM AMA transiently increased $O_2\cdot$- level at 25 min. All the tested doses of AMA increased $O_2\cdot$- levels at 180 min. The increased $O_2\cdot$- levels in AMA-treated HPF cells probably resulted from the enhanced production of $O_2\cdot$- itself rather than the reduction of SOD activity because MMP ($\Delta\Psi_m$) loss was dose-dependently observed in these cells and the expression of SOD1 and SOD2 were not downregulated by AMA. Moreover, it is likely that 200 μM AMA directly damaged mitochondria and increased the generation of $O_2\cdot$- at 25 min, consequently resulting in an increase in ROS (DCF) levels at the early time phases of 25-180 min. TXN and TXNRs can stimulate cell proliferation and confer resistance to anticancer drugs (26,27). Our results showed that AMA downregulated TXN and TXNR2 levels. Therefore, the downregulation of TXN and TXNR2 due to treatment with AMA might make HPF cells more sensitive to this agent. In addition, it seems that AMA altered the levels of SOD2 and TXNR2 in the mitochondria of HPF cells since these antioxidant enzymes specifically maintain the redox state in mitochondria.

NAC generally attenuated ROS levels in AMA-treated or -untreated HPF cells. It also prevented cell growth inhibition, apoptosis and MMP ($\Delta\Psi_m$) loss in 100 or 200 μM AMA-treated HPF cells. Interestingly, NAC induced necrotic cell death in 200 μM AMA-treated HPF cells. In addition, 5 mM NAC strongly induced necrotic cell death in 200 μM AMA-treated HPF cells, and it decreased ROS (DCF) levels, but strongly increased $O_2\cdot$- level in these cells (data not shown). Treatment with 2 or 5 mM NAC was likely to change cell death pathway (switching apoptotic cell death to necrotic cell death) in 200 μM AMA-treated HPF cells via affecting different ROS levels (DCF or DHE levels). In addition, the other antioxidant vitamin C slightly attenuated ROS (DCF) level in 100 or 200 μM AMA-treated HPF cells. Interestingly, vitamin C enhanced cell growth inhibition, apoptosis and MMP ($\Delta\Psi_m$) loss in 100 μM AMA-treated HPF cells and increased $O_2\cdot$- level in these cells. However, vitamin C strongly attenuated $O_2\cdot$- level in 200 μM AMA-treated HPF cells and this agent reduced growth inhibition, apoptosis and MMP ($\Delta\Psi_m$) loss in these cells. The change of $O_2\cdot$- level rather than ROS (DCF) level due to vitamin C seemed to be more closely related to AMA-induced HPF cell death. These results implied that vitamin C can be an oxidant or an antioxidant in HPF cells depending on the doses of AMA. Although vitamin C possesses strong antioxidant properties, the mechanism underlying these properties is still unclear *in vivo* and *in vitro* (28,29). Z-VAD did not significantly change ROS and cell death levels in AMA-treated HPF cells. BSO showing a slight increase in HPF cell death by 100 μM AMA increased strongly ROS (DCF) level, but this agent did not affect ROS level and cell death in 200 μM AMA-treated HPF cells. Collectively, AMA-induced HPF cell death is tightly correlated with the generation of ROS. BSO alone induced cell death in HPF control cells which was accompanied by the production ROS including $O_2\cdot$-. Therefore, ROS increased by BSO might be related to HPF cell death (30,31).

AMA increased the number of GSH-depleted cells in HPF cells. As expected, NAC showing an anti-apoptotic effect on AMA-treated HPF cells significantly prevented GSH depletion in these cells. In addition, vitamin C augmented GSH depletion in 100 μM AMA-treated HPF cells and this agent attenuated the depletion induced by treatment with 200 μM AMA. BSO showing non-effects on AMA-induced HPF cell death did not change GSH depleted cell number in these cells. These results suggest that the intracellular GSH content has a decisive role on AMA-induced HPF cell death. It is of note that BSO did not significantly affect GSH contents in AMA-treated or -untreated HPF cells. However, our previous reports demonstrate that BSO enhanced GSH depletion as well as cell death in AMA-treated Calu-6 cells (32) and gallic acid-treated HPF cells (33). These data imply that BSO differently influences GSH content levels depending on cell types. The decreased GSH levels in AMA-treated HPF cells at the early time phases (25-90 min) probably resulted from its consumption against increased ROS levels by AMA. On the whole, GSH and ROS levels were inversely related in AMA-treated HPF cells, implying that GSH and ROS in these cells influence each other in the early time-points.

In conclusion, AMA inhibited the growth of HPF cells via apoptosis as well as a G1 phase arrest of the cell cycle. AMA-induced HPF cell death was related to increases in ROS level and GSH depletion. Our current results provide practical information to appreciate the cellular effect of AMA on normal lung cells in relation to ROS and GSH.

Acknowledgements

This study was supported by a grant from the National Research Foundation of Korea (NRF) funded by the Korean government (MSIP; no. 2008 0062279) and supported by the Basic Science Research Program through the NRF funded by the Ministry of Education (no. 2013006279).

References

1. Zorov DB, Juhaszova M and Sollott SJ: Mitochondrial ROS-induced ROS release: An update and review. Biochim Biophys Acta 1757: 509-517, 2006.
2. Zelko IN, Mariani TJ and Folz RJ: Superoxide dismutase multigene family: A comparison of the CuZn-SOD (SOD1), Mn-SOD (SOD2), and EC-SOD (SOD3) gene structures, evolution, and expression. Free Radic Biol Med 33: 337-349, 2002.
3. Wilcox CS: Reactive oxygen species: Roles in blood pressure and kidney function. Curr Hypertens Rep 4: 160-166, 2002.
4. Marks PA: Thioredoxin in cancer - role of histone deacetylase inhibitors. Semin Cancer Biol 16: 436-443, 2006.
5. Alexandre A and Lehninger AL: Bypasses of the antimycin a block of mitochondrial electron transport in relation to ubisemiquinone function. Biochim Biophys Acta 767: 120-129, 1984.
6. Campo ML, Kinnally KW and Tedeschi H: The effect of antimycin A on mouse liver inner mitochondrial membrane channel activity. J Biol Chem 267: 8123-8127, 1992.
7. Balaban RS, Nemoto S and Finkel T: Mitochondria, oxidants, and aging. Cell 120: 483-495, 2005.
8. Panduri V, Weitzman SA, Chandel NS and Kamp DW: Mitochondrial-derived free radicals mediate asbestos-induced alveolar epithelial cell apoptosis. Am J Physiol Lung Cell Mol Physiol 286: L1220-L1227, 2004.
9. Petronilli V, Penzo D, Scorrano L, Bernardi P and Di Lisa F: The mitochondrial permeability transition, release of cytochrome *c* and cell death. Correlation with the duration of pore openings in situ. J Biol Chem 276: 12030-12034, 2001.
10. Pastorino JG, Tafani M, Rothman RJ, Marcinkeviciute A, Hoek JB and Farber JL: Functional consequences of the sustained or transient activation by Bax of the mitochondrial permeability transition pore. J Biol Chem 274: 31734-31739, 1999.
11. Park WH, Han YW, Kim SH and Kim SZ: An ROS generator, antimycin A, inhibits the growth of HeLa cells via apoptosis. J Cell Biochem 102: 98-109, 2007.
12. Park WH, Han YW, Kim SW, Kim SH, Cho KW and Kim SZ: Antimycin A induces apoptosis in As4.1 juxtaglomerular cells. Cancer Lett 251: 68-77, 2007.
13. King MA: Antimycin A-induced killing of HL-60 cells: Apoptosis initiated from within mitochondria does not necessarily proceed via caspase 9. Cytometry A 63: 69-76, 2005.
14. Guha G, Mandal T, Rajkumar V and Ashok Kumar R: Antimycin A-induced mitochondrial apoptotic cascade is mitigated by phenolic constituents of *Phyllanthus amarus* aqueous extract in Hep3B cells. Food Chem Toxicol 48: 3449-3457, 2010.
15. You BR and Park WH: The effects of antimycin A on endothelial cells in cell death, reactive oxygen species and GSH levels. Toxicol In Vitro 24: 1111-1118, 2010.
16. Han YH and Park WH: Growth inhibition in antimycin A treated-lung cancer Calu-6 cells via inducing a G1 phase arrest and apoptosis. Lung Cancer 65: 150-160, 2009.
17. Han YH, Kim SH, Kim SZ and Park WH: Antimycin A as a mitochondrial electron transport inhibitor prevents the growth of human lung cancer A549 cells. Oncol Rep 20: 689-693, 2008.
18. Han YH and Park WH: Tiron, a ROS scavenger, protects human lung cancer Calu-6 cells against antimycin A-induced cell death. Oncol Rep 21: 253-261, 2009.
19. Han YH, Kim SZ, Kim SH and Park WH: Pyrogallol inhibits the growth of lung cancer Calu-6 cells via caspase-dependent apoptosis. Chem Biol Interact 177: 107-114, 2009.
20. You BR and Park WH: Gallic acid-induced lung cancer cell death is related to glutathione depletion as well as reactive oxygen species increase. Toxicol In Vitro 24: 1356-1362, 2010.
21. You BR, Kim SH and Park WH: Reactive oxygen species, glutathione, and thioredoxin influence suberoyl bishydroxamic acid-induced apoptosis in A549 lung cancer cells. Tumour Biol 36: 3429-3439, 2015
22. You BR, Shin HR, Han BR and Park WH: PX-12 induces apoptosis in Calu-6 cells in an oxidative stress-dependent manner. Tumour Biol 36: 2087-2095, 2015.
23. Jia L, Allen PD, Macey MG, Grahn MF, Newland AC and Kelsey SM: Mitochondrial electron transport chain activity, but not ATP synthesis, is required for drug-induced apoptosis in human leukaemic cells: A possible novel mechanism of regulating drug resistance. Br J Haematol 98: 686-698, 1997.
24. Han YH, Kim SH, Kim SZ and Park WH: Antimycin A as a mitochondria damage agent induces an S phase arrest of the cell cycle in HeLa cells. Life Sci 83: 346-355, 2008.
25. Han YW, Kim SZ, Kim SH and Park WH: The changes of intracellular H_2O_2 are an important factor maintaining mitochondria membrane potential of antimycin A-treated As4.1 juxtaglomerular cells. Biochem Pharmacol 73: 863-872, 2007.
26. Gallegos A, Gasdaska JR, Taylor CW, Paine-Murrieta GD, Goodman D, Gasdaska PY, Berggren M, Briehl MM and Powis G: Transfection with human thioredoxin increases cell proliferation and a dominant-negative mutant thioredoxin reverses the transformed phenotype of human breast cancer cells. Cancer Res 56: 5765-5770, 1996.
27. Kim SJ, Miyoshi Y, Taguchi T, Tamaki Y, Nakamura H, Yodoi J, Kato K and Noguchi S: High thioredoxin expression is associated with resistance to docetaxel in primary breast cancer. Clin Cancer Res 11: 8425-8430, 2005.
28. Poljsak B and Raspor P: The antioxidant and pro-oxidant activity of vitamin C and trolox in vitro: A comparative study. J Appl Toxicol 28: 183-188, 2008.
29. Halliwell B: Vitamin C: Antioxidant or pro-oxidant in vivo? Free Radic Res 25: 439-454, 1996.
30. Estrela JM, Ortega A and Obrador E: Glutathione in cancer biology and therapy. Crit Rev Clin Lab Sci 43: 143-181, 2006.
31. Higuchi Y: Glutathione depletion-induced chromosomal DNA fragmentation associated with apoptosis and necrosis. J Cell Mol Med 8: 455-464, 2004.
32. Han YH and Park WH: The effects of N-acetyl cysteine, buthionine sulfoximine, diethyldithiocarbamate or 3-amino-1,2,4-triazole on antimycin A-treated Calu-6 lung cells in relation to cell growth, reactive oxygen species and glutathione. Oncol Rep 22: 385-391, 2009.
33. Park WH and You BR: Enhancement of gallic acid-induced human pulmonary fibroblast cell death by N-acetyl cysteine and L-buthionine sulfoximine. Hum Exp Toxicol 30: 992-999, 2011.